Continuous-Variable Triple-Photon States Quantum Entanglement

E. A. Rojas González,[1,2] A. Borne,[3,4] B. Boulanger,[4] J. A. Levenson,[1] and K. Bencheikh[1,*]
[1]Centre de Nanosciences et de Nanotechnologies CNRS/Université Paris-Saclay, 91460 Marcoussis, France
[2]Department of Engineering Sciences, The Ångström Laboratory, Uppsala University, SE-75121 Uppsala, Sweden
[3]Weizmann Institutes of Science, Rehovot 7610001, Israel
[4]Institut Néel, CNRS/Université Grenoble Alpes, 38402 Grenoble, France

(Received 7 June 2017; revised manuscript received 17 October 2017; published 22 January 2018)

We investigate the quantum entanglement of the three modes associated with the three-photon states obtained by triple-photon generation in a phase-matched third-order nonlinear optical interaction. Although the second-order processes have been extensively dealt with, there is no direct analogy between the second and third-order mechanisms. We show, for example, the absence of quantum entanglement between the quadratures of the three modes in the case of spontaneous parametric triple-photon generation. However, we show robust, seeding-dependent, genuine triple-photon entanglement in the fully seeded case.

DOI: 10.1103/PhysRevLett.120.043601

Introduction.—Twin-photon states have deeply influenced the history of quantum optics and are the main ingredient in several quantum protocols. Their ubiquity contrasts with the case of triple-photon states (TPS). The unique quantum properties of TPS were anticipated in the seminal paper on GHZ states [1]. Their tripartite entanglement is identified as a direct way to contradict local realism theory for nonstatistical predictions of quantum mechanics. Later on, *W* states have been predicted to retain maximally bipartite entanglement when any one of the three qubits is traced out [2]. Very recently, anisotropy was identified as a new invariant for pure three-qubit states and was found identical for each of their pairs, opening several promising applications [3]. More generally, one can expect that TPS plays in quantum optics a similar role as twin-photon states did over the last 40 years and allow the development of novel and efficient quantum protocols based on triple-photon entanglement or announced entangled twins. This is provided that clever optimization of both material and nonlinear interaction is achieved to overcome the weakness of third-order nonlinear processes. Until now, only configurations based on second-order nonlinear interactions have succeeded in producing TPS [4–8] at the expense of increased complexity, low efficiency, or detection conditioned protocols preventing their use. In the continuous variable (CV) domain, tripartie full inseparability was demonstrated by Aoki *et al.* in 2003 [9] using linear optics and squeezed states. Very recently, an important step was accomplished by Armstrong *et al.*, demonstrating CV TPS exhibiting genuine three-body entanglement [10]. However, the most direct way to produce TPS is in pure $\chi^{(3)}$ materials, in which a pump photon $\hbar\omega_p$ is down-converted simultaneously into a triplet $\hbar\omega_1$, $\hbar\omega_2$, and $\hbar\omega_3$ with the subsequent energy conservation, $\hbar\omega_p = \hbar\omega_1 + \hbar\omega_2 + \hbar\omega_3$, and momentum conservation $\hbar\vec{k}_p = \hbar\vec{k}_1 + \hbar\vec{k}_2 + \hbar\vec{k}_3$. In the degenerate configuration, $\chi^{(3)}$-based TPS exhibit negativities in the Wigner function [11], signature of non-Gaussian statistics, constituting a real asset over TPS obtained by cascaded $\chi^{(2)}$ interactions and linear optics. Only one experimental demonstration of triple-photon generation (TPG) was reported in the regime of bistate seeding; i.e., two of the three fields associated with the outcoming component of the triple-photons are injected together with the pump field [12]. This pioneering work clearly demonstrates a phase-matched third-order nonlinear process. Its transposition to spontaneous down-conversion is, however, precluded by the small $\chi^{(3)}$ value. For instance, in the fluorescence regime, less than 0.01 triplet per day is expected [11]. There is an active research for novel materials and geometrical configurations pushing nowadays the efficiency of the reverse nonlinear process, namely third-harmonic generation, from bulk to waveguide operation [13–16]. One can reasonably conjecture this will contribute to increased TPG efficiency as predicted by semiclassical theories [17–19]. However, one can wonder if our comprehension at the quantum level of the process is sufficient to optimize the interaction. Until now, this optimization is strongly driven by the analogy with the well-known and largely investigated $\chi^{(2)}$ process.

In this Letter, we develop a full quantum description of TPS in the CV domain. To the best of our knowledge, the CV quantum properties [20] remain unexplored for TPS generated by a pure third-order nonlinear interaction. We discuss spontaneous, single, double, and triple-seeded configurations and demonstrate that using twin-photon knowledge is often a wrong strategy for TPS optimization. As a result, no entanglement is found in the spontaneous emission regime. More importantly, tripartite entanglement is predicted in the triple seeding configuration and is found strongly increasing with the seeding, becoming a novel avenue for TPS optimization.

The starting point of our theoretical analysis is the interaction Hamiltonian describing TPG in a $\chi^{(3)}$ material [21]. It reduces to

$$\hat{H} = \hbar\kappa(\hat{a}_1^\dagger \hat{a}_2^\dagger \hat{a}_3^\dagger + \hat{a}_1 \hat{a}_2 \hat{a}_3), \tag{1}$$

for a monochromatic strong undepleted classical pump. κ is proportional to the pump amplitude and to the nonlinear susceptibility $\chi^{(3)}$. The annihilation operators $\hat{a}_k$ ($k = 1, 2, 3$) describe the triple photons modes. We now consider the evolution of the operators in the Heisenberg picture

$$\frac{d\hat{a}_k(t)}{dt} = \frac{\imath}{\hbar}[\hat{H}, \hat{a}_k(t)]. \tag{2}$$

Let $\hat{A}_k$ ($\hat{A}_k^\dagger$) be the annihilation (creation) operators of mode k after the nonlinear interaction. We define the amplitude and phase quadratures $\hat{p}_k = \hat{A}_k + \hat{A}_k^\dagger$ and $\hat{q}_k = \imath(\hat{A}_k - \hat{A}_k^\dagger)$, satisfying the canonical commutation relations $[\hat{q}_k, \hat{p}_k] = 2\imath$. Their quantum fluctuations are measured with balanced homodyne detections. By sweeping the phase θ_k of the local oscillator, one has access to the generalized quadratures $\hat{P}_k(\theta_k) = e^{-\imath\theta_k}\hat{A}_k^\dagger + e^{\imath\theta_k}\hat{A}_k$ and $\hat{Q}_k(\theta_k) = \hat{P}_k(\theta_k + \pi/2)$. Let us finally define the following linear combinations:

$$\begin{aligned} \hat{u} &= h_1\hat{P}_1 + h_2\hat{P}_2 + h_3\hat{P}_3, \\ \hat{v} &= g_1\hat{Q}_1 + g_2\hat{Q}_2 + g_3\hat{Q}_3, \end{aligned} \tag{3}$$

where h_k and g_k are arbitrary real parameters introduced experimentally as attenuations or amplifications of the photocurrents generated by the balanced homodyne detections. Phase dependence is intentionally omitted in Eq. (3) for simplicity. We quantify multibody quantum entanglement of TPS using the nonseparability criterion S introduced by van Loock and Furusawa in Ref. [22], defined as

$$S = \langle \Delta\hat{u}^2 \rangle + \langle \Delta\hat{v}^2 \rangle, \tag{4}$$

which can be measured experimentally using homodyne detection. Expanding Eq. (4) and using Eq. (3) we find

$$\begin{aligned} S = &\sum_{k=1}^{3} h_k^2 \langle \Delta\hat{Q}_k^2 \rangle + \sum_{k=1}^{3} g_k^2 \langle \Delta\hat{P}_k^2 \rangle, \\ &+ \sum_{k=1}^{3}\sum_{\substack{m=1 \\ m\neq k}}^{3} h_k h_m (\langle \hat{Q}_k \hat{Q}_m \rangle - \langle \hat{Q}_k \rangle \langle \hat{Q}_m \rangle), \\ &+ \sum_{k=1}^{3}\sum_{\substack{m=1 \\ m\neq k}}^{3} g_k g_m (\langle \hat{P}_k \hat{P}_m \rangle - \langle \hat{P}_k \rangle \langle \hat{P}_m \rangle). \end{aligned} \tag{5}$$

The two first terms are the sum of the quadrature variances. The two last describe cross correlations between the output modes at the origin of the entanglement. Indeed, whereas the two first terms are always positive, the two last can be negative and can interfere destructively with the first ones. The criterion S is a function of h_k and g_k. If

$$S < f_p = 2(|h_k g_k| + |h_l g_l + h_m g_m|) \tag{6}$$

for a given permutation $\{k, l, m\}$ of $\{1, 2, 3\}$, then the quantum system is said to be fully inseparable [22]. The system is at least partially separable if $f_p \leq S < f_s = 2(|h_k g_k| + |h_l g_l| + |h_m g_m|)$. According to [22], the parameters h_k and g_k are chosen such that $[\hat{u}, \hat{v}] = 0$, to allow $S \to 0$ and the existence of simultaneous eigenstates of $\hat{u}$ and $\hat{v}$. As pointed out by Teh and Reid [23], one has to distinguish between full inseparability and genuine entanglement. They both are equivalent only for pure quantum states, otherwise, for mixed states, full inseparability is not a sufficient condition to claim entanglement. One has instead to fulfill

$$\begin{aligned} S < 2 \ \min\{&|h_1 g_1| + |h_2 g_2 + h_3 g_3|, \\ &|h_2 g_2| + |h_1 g_1 + h_3 g_3|, |h_3 g_3| + |h_1 g_1 + h_2 g_2|\}, \end{aligned} \tag{7}$$

to confirm genuine entanglement—condition (18) in [23]—which is more stringent than criterion (6). In the subsequent analysis, the boundaries in (6) and (7) are, respectively, 4 and 2 for our chosen $\hat{u}$ and $\hat{v}$ quadratures (and hence h_k and g_k) in the case of doubly or fully seeded TPG. We can thus claim genuine entanglement when $S < 2$ or at least full inseparability when $S < 4$.

The determination of S for TPS relies on the resolution of Eq. (2). Unfortunately, no analytical solutions are known in the frame of quantum mechanics, though their exact classical solutions are Jacobi elliptic functions [24]. Here, to obtain an approximate solution of the operators at a time t, we use the Baker-Hausdorff expansion

$$\hat{A}_k = \hat{a}_k + \sum_{n=1}^{\infty} \frac{(\imath\xi)^n}{n!} \hat{\Omega}_{n;klm}, \tag{8}$$

to a finite order, $\xi = \kappa t$ being the interaction strength and

$$\hat{\Omega}_{n;klm} = \frac{1}{(\hbar\kappa)^n} [\underbrace{\hat{H}, [\hat{H}, [\cdots \hat{H}, [\hat{H}}_{n\text{-times}}, \hat{a}_k]]]], \tag{9}$$

with $\{k, l, m\}$ being permutations of $\{1, 2, 3\}$. The expansion order of the operators in Eq. (8) is crucial for the validity of our analysis. It depends on the interaction strength ξ and on the average photon number of the seeding. In the following, we will analyze different situations of TPG expanding Eq. (8) to a finite order and calculate the criterion S using a combination of both symbolic and numerical computational methods. For all numerical analysis we take $|\xi| = 1.75 \times 10^{-6}$, deduced

from [24], which is very representative of the third-order nonlinearity of nowadays materials.

Triple-photon parametric fluorescence.—In the fluorescence case, there is no seeding and since $|\xi| \ll 1$, the expansion is valid at any order. It is well known that spontaneous parametric down-conversion (SPDC) induces strong quantum entanglement between the twin modes. Surprisingly, our analysis shows that spontaneous TPG does not exhibit such quantum entanglement in the CV regime for any chosen quadratures $\hat{u}$ and $\hat{v}$. The cross correlation terms in Eq. (5) between the output modes vanish and S reduces to

$$S = (1 + 2\langle \hat{A}^\dagger \hat{A} \rangle) \sum_{k=1}^{3} (h_k^2 + g_k^2), \tag{10}$$

when assuming identical average photon number $\langle \hat{A}^\dagger \hat{A} \rangle$ in each mode. The full derivation of Eq. (10) is given in the Supplemental Material [25]. According to Eq. (10), the criterion S only depends on h_k, g_k and on ξ, which is contained in $\langle \hat{A}^\dagger \hat{A} \rangle$. We compare the result given by Eq. (10) to the classical limit f_s by analyzing the difference $S - f_s$. After some mathematical manipulations, we end up with $S - f_s = 2\Gamma^2 \langle \hat{A}^\dagger \hat{A} \rangle + \sum_{k=1}^{3} (|h_k| - |g_k|)^2$, where $\Gamma^2 = (h_1^2 + h_2^2 + h_3^2 + g_1^2 + g_2^2 + g_3^2)$. Each term being positive, $S \geq f_s$ for any choice of h_k and g_k. This result clearly demonstrates that, in contrast to SPDC, the three modes are fully independent, meaning that their quantum fluctuations are totally uncorrelated. This result could be easily understood as follows. The triplets are generated from the vacuum quantum fluctuations as the twins. However, for a given eigenvalue outcome of the observable, $\hat{Q}_1$ for example, the two others, $\hat{Q}_2$ and $\hat{Q}_3$, can still take any random pair of eigenvalues. Each realization is thus independent from the previous one.

Partially seeded triple-photon generation.—The validity of our analysis in the seeded cases is discussed in detail in the Supplemental Material [25]. We show that a sufficient condition for the expansion to be valid is $|\xi\alpha| \ll 1$, where $\bar{N}_{\text{in}} = |\alpha|^2$ is the incident average photon number per mode. All subsequent numerical analyses are done using $\bar{N}_{\text{in}} \leq 10^{11}$ and a fifth-order expansion of the operators $\hat{A}_k$. The associated errors on the operators is about 6.4% and even smaller on the estimation of the gains, variances, and S.

When only one of the three modes is excited by a bright coherent state $|\alpha\rangle$ containing $\bar{N}_{\text{in}}$ photons on average, no three-body quantum entanglement was found. If, for example, mode 3 is seeded, we can replace the operator $\hat{a}_3$ by its classical field amplitude counterpart $\imath E_3$, chosen to be complex for convenience, assuming that E_3 is a real number. The Hamiltonian becomes $\hat{H}^{(2)} = \imath\hbar\kappa(\hat{a}_1\hat{a}_2 - \hat{a}_1^\dagger\hat{a}_2^\dagger)$, where $\kappa = gE_3$. It describes SPDC, where a pump photon is converted into twin photons. In the third-order configuration, however, the down-conversion process is proportional to the effective second-order susceptibility $\chi^{(3)}E_3$, meaning that the efficiency depends on the seeding level.

Figure 1 allows us to analyze the bipartite nonseparability criterion S for these twins. The magenta continuous line with the (plus) markers shows S for modes 1 and 2, using the quadratures $\hat{u} = \hat{Q}_1 + \hat{Q}_2$ and $\hat{v} = \hat{P}_1 - \hat{P}_2$, as a function of the seeding average photon number in mode 3. The quadratures are determined from the exact solutions of Eq. (2) using $\hat{H}^{(2)}$. S starts at 4, which is the classical limit, i.e. the sum of the four quadrature variances, then decreases as the seeding gets stronger. The gray area beneath $S = 2$ indicates the quantum region, meaning that the measurement of the quadrature $\hat{Q}_2$ (respectively, $\hat{P}_2$) allows us to know $\hat{Q}_1$ (respectively, $\hat{P}_1$) better than the standard quantum limit, the shot noise of a coherent state [26]. Figure 1 shows that the entanglement gets stronger as the seeding increases. In a sense, the single mode seeded TPG is a reconfigurable two-body entanglement source where the seeded mode acts as a control parameter: it changes the strength of the interaction and selects which quadratures are entangled depending on the seeding phase. When $E_3 \to 0$, it reaches the fluorescence case, which can be seen as an effective second-order process driven by the quantum fluctuations of mode 3. This reasoning helps us to understand the origin of the missing three-body quantum

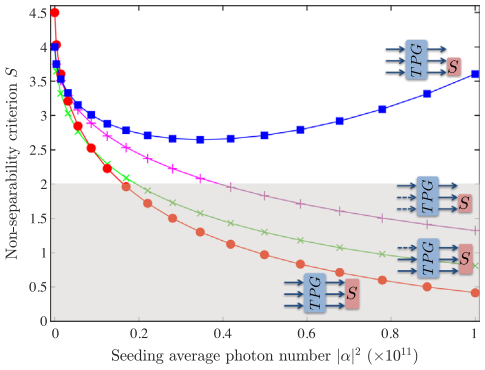

FIG. 1. Evolution of the nonseparability criterion S as a function of the seeding average photon number for $|\xi| = 1.75 \times 10^{-6}$ and for different injection cases. The gray area highlights the quantum region of tripartite genuine entanglement. Full inseparability is fulfilled between 2 and 4. The triple-photon generation boxes show the different schemes with the seeded (full arrows) and nonseeded (dashed arrows) modes. The S boxes indicate the modes concerned by the S measurement. Magenta line with (plus) markers: single seeding case. Green line with (times) markers: double seeding case. Red line with (circle) markers for the fully seeded at $\theta_1 = 0$, $\theta_2 = \theta_3 = \pi$, and for $\beta = \sqrt{2}$. The phase of the seeding coherent state is $\phi = \pi/2$. Blue line with (square) markers: same as the red curve but for quadratures $\hat{u} = \hat{Q}_1 + \hat{Q}_2$ and $\hat{v} = \hat{P}_1 - \hat{P}_2$.

entanglement. Indeed, each eigenvalue resulting from the measurement of the seeding mode, even at shot noise, will reset the twin-photon generation process.

The case of two modes seeded TPG, corresponding to the arrangement described in [24], is analyzed hereafter. The input state of the system is $|\psi\rangle = |0_1, \alpha_2, \alpha_3\rangle$. The most trivial combinations to be considered in Eq. (3) are for $h_1 = g_1 = 1$, $h_2 = h_3 = 1/\sqrt{2}$, and $g_2 = g_3 = -1/\sqrt{2}$. All the local oscillator phases are $\theta_k = 0$. Any other phase does not influence the result except by shifting the minimum value of S in the phase space. The chosen parameters suggest that the noninjected mode 1 is investigated through the measurement of both seeded modes 2 and 3. The green line with (times) markers in Fig. 1 represents the corresponding S. Starting at 4, it decreases as the seeding grows, violating condition (6) and showing that the three modes are fully inseparable. At $\bar{N}_{\rm in} \simeq 2 \times 10^{10}$, S goes below 2, indicating genuine tripartite entanglement according to Eq. (7). In this regime, measuring both modes 2 and 3 is necessary to know mode 1 better than the standard quantum limit.

Fully seeded triple-photon generation.—This section focuses on the case where the three modes are initially excited. The input state of the system is $|\psi\rangle = |\alpha_1, \alpha_2, \alpha_3\rangle$. As for the fully seeded second-order parametric interaction, it is necessary to consider the phase of the different modes at the input relative to the pump phase. We consider identical coherent states seeding the three modes, so that $\alpha_k = |\alpha| e^{\imath\phi}$ for each mode.

We start by looking at the evolution of the gain $G = \bar{N}_{\rm out}/\bar{N}_{\rm in}$, where $\bar{N}_{\rm out} = \langle \hat{A}_k^\dagger \hat{A}_k \rangle$ and $\bar{N}_{\rm in} = \langle \hat{a}_k^\dagger \hat{a}_k \rangle$ are the output and input average photon number in each mode. We also calculate the variance of the quadratures $\hat{P}_k$ and $\hat{Q}_k$. Figure 2(a) represents the gain G for $\bar{N}_{\rm in} = 4 \times 10^{10}$ in polar coordinates as a function of the phase ϕ of the seeding. It shows amplification ($G > 1$) and deamplification ($G < 1$) regimes and features three lobs subsequent to the $e^{\imath 3\phi}$ dependance of $\bar{N}_{\rm out}$. The maxima are located at $\phi = \pi/2, 7\pi/6$ and $11\pi/6$ corresponding to the phases for

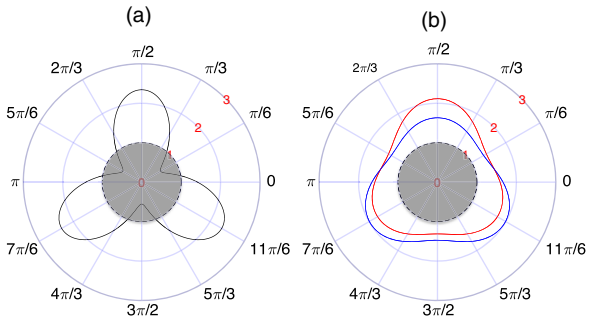

FIG. 2. Gain (a) and $\hat{P}_k$ (red) and $\hat{Q}_k$ (blue) variances (b) as a function of the phase of the seeding fields, for $|\xi| = 1.75 \times 10^{-6}$ and $\bar{N}_{\rm in} = 4 \times 10^{10}$. The gray circles indicate the unity gain in (a) and the standard quantum limit in (b).

which the down-conversion TPG process $\omega_p \to \omega_1 + \omega_2 + \omega_3$ is enhanced. The minima are obtained for $\phi = \pi/6$, $5\pi/6$ and $3\pi/2$. Here, it is the sum frequency process $\omega_1 + \omega_2 + \omega_3 \to \omega_p$ which predominates. Figure 2(b) shows the variances of the quadratures $\hat{P}_k$ (red) and $\hat{Q}_k$ (blue) in the same conditions of Fig. 2(a). The most interesting feature, besides the presence of the three lobes, is that the variances are always above the shot noise (gray circle) when the modes are measured separately. This behavior is equivalent to nondegenerate twin-photon generation where signal and idler modes exhibit super-Poissonian fluctuations, when taken separately, and Einstein-Podolsky-Rosen entanglement when combined [26].

Looking for tripartite quantum entanglement, we consider the following particular linear combinations of the operators of Eq. (3):

$$\hat{u} = \hat{Q}_1 + \frac{1}{\beta\sqrt{2}}(\hat{Q}_2 + \hat{Q}_3),$$
$$\hat{v} = \hat{P}_1 - \beta\frac{1}{\sqrt{2}}(\hat{P}_2 + \hat{P}_3). \tag{11}$$

The extra parameter β allows further optimization. Our analysis shows that for each phase θ_1 of the local oscillator used for detecting mode 1, there exists a couple of phases θ_2 and θ_3 for modes 2 and 3 that minimize S. The red line with (circle) markers in Fig. 1 shows the evolution of S as a function of $\bar{N}_{\rm in}$. It is obtained in the amplification regime and for $\theta_1 = 0$ and $\theta_2 = \theta_3 = \pi$. As the seeding increases, the red curve goes rapidly below 4, satisfying the full inseparability condition and then goes below 2 at $\bar{N}_{\rm in} \simeq 1.8 \times 10^{10}$, showing genuine three-body quantum entanglement. This means that a measurement of both modes 2 and 3 is necessary to gain information on mode 1 better than the shot noise limit. Indeed, if one tries to determine mode 1 using only mode 2, for example, through the quadratures $\hat{u} = \hat{Q}_1 + \hat{Q}_2$ and $\hat{v} = \hat{P}_1 - \hat{P}_2$, then $S > 2$, as shown by the blue line with (square) markers in Fig. 1.

The feasibility and the likelihood of reaching the quantum level is an important aspect. The parameters considered in these calculations are compatible with existing experimental results at the classical level for bulk materials of [24], from which the interaction strength $|\xi| = 1.75 \times 10^{-6}$ is deduced. Moreover, the seeding average photon number in our calculations is 2 orders of magnitude smaller than in [24]. Concerning the crucial issue of losses, which degrade the quantum correlations, they are discussed in the Supplemental Material [25]. They are modeled by beam splitters with a transmission coefficient $T = \eta$ in front of ideal detection systems, where η is the overall quantum efficiency per mode. We show for the fully seeded TPG, genuine tripartite entanglement preservation up to 38% losses per mode. Such robustness against losses is due to the excess noise of the three modes as depicted in Fig. 2(b).

Conclusion.—In our analysis of parametric TPG, some counterintuitive results are found when comparing with the well-known twin-photon second-order equivalent. The first counterintuitive result is obtained for the pure spontaneous case for which we demonstrate the lack of tripartite quantum entanglement. The more important finding is for the fully seeded TPG. It exhibits a phase-dependent gain, behaving similarly to the well-known second-order phase-sensitive parametric amplifier. But it also appears as an efficient way to generate genuine tripartite CV quantum entanglement. An additional property corresponds to the increase in efficiency with the amplitude of the seeding. Finally, our pure triple-photon generation approach for generating TPS is done in a traveling wave configuration which is very practical for subsequent quantum information protocols. Moreover, it is more robust against losses than the $\chi^{(2)}$-based TPS. Indeed, instead of using squeezed beams, we deal with super-Poissonian states known to be very insensitive to optical losses. In conclusion, this three-body genuine quantum entanglement based on a true triple-photon generation constitutes a real asset for a new generation quantum cryptography and other quantum information protocols based on multipartite entanglement.

This work is supported by the French Agence Nationale de la Recherche through the project TRIQUI (ANR-17-CE24-0041-03).

*kamel.bencheikh@c2n.upsaclay.fr

[1] D. M. Greenberger, M. A. Horne, A. Shimony, and A. Zeilinger, Am. J. Phys. **58**, 1131 (1990).
[2] W. Dür, G. Vidal, and J. I. Cirac, Phys. Rev. A **62**, 062314 (2000).
[3] S. Cheng and M. J. W. Hall, Phys. Rev. Lett. **118**, 010401 (2017).
[4] D. Bouwmeester, J.-W. Pan, M. Daniell, H. Weinfurter, and A. Zeilinger, Phys. Rev. Lett. **82**, 1345 (1999).
[5] A. S. Coelho, F. A. S. Barbosa, K. N. Cassemiro, A. S. Villar, M. Martinelli, and P. Nussenzveig, Science **326**, 823 (2009).
[6] H. Hübel, D. R. Hamel, A. Fedrizzi, S. Ramelow, K. J. Resch, and T. Jennewein, Nature (London) **466**, 601 (2010).
[7] L. K. Shalm, D. R. Hamel, Z. Yan, C. Simon, K. J. Resch, and T. Jennewein, Nat. Phys. **9**, 19 (2013).
[8] D. R. Hamel, L. K. Shalm, H. Hübel, A. J. Miller, F. Marsili, V. B. Verma, R. P. Mirin, S. W. Nam, K. J. Resch, and T. Jennewein, Nat. Photonics **8**, 801 (2014).
[9] T. Aoki, N. Takei, H. Yonezawa, K. Wakui, T. Hiraoka, A. Furusawa, and P. van Loock, Phys. Rev. Lett. **91**, 080404 (2003).
[10] S. Armstrong, M. Wang, R. Y. Teh, Q. Gong, Q. He, J. Janousek, H.-A. Bachor, M. D. Reid, and P. K. Lam, Nat. Phys. **11**, 167 (2015).
[11] K. Bencheikh, F. Gravier, J. Douady, J. A. Levenson, and B. Boulanger, C.R. Phys. **8**, 206 (2007).
[12] J. Douady and B. Boulanger, Opt. Lett. **29**, 2794 (2004).
[13] A. Efimov, A. J. Taylor, F. G. Omenetto, J. C. Knight, W. J. Wadsworth, and P. S. J. Russell, Opt. Express **11**, 2567 (2003).
[14] K. Bencheikh, S. Richard, G. Mélin, G. Krabshuis, F. Gooijer, and J. A. Levenson, Opt. Lett. **37**, 289 (2012).
[15] A. Cavanna, F. Just, X. Jiang, G. Leuchs, M. V. Chekhova, P. S. Russell, and N. Y. Joly, Optica **3**, 952 (2016).
[16] S. C. Warren-Smith, J. Wie, M. Chemnitz, R. Kostecki, H. Ebendorff-Heidepriem, T. M. Monro, and M. A. Schmidt, Opt. Express **24**, 17860 (2016).
[17] S. Richard, K. Bencheikh, B. Boulanger, and J. A. Levenson, Opt. Lett. **36**, 3000 (2011).
[18] M. Corona, K. Garay-Palmett, and A. B. U'ren, Opt. Lett. **36**, 190 (2011).
[19] M. Corona, K. Garay-Palmett, and A. B. U'Ren, Phys. Rev. A **84**, 033823 (2011).
[20] S. L. Braunstein and A. K. Pati, *Quantum Information with Continuous Variables* (Springer Science & Business Media, New York, 2012).
[21] A. Dot, A. Borne, B. Boulanger, K. Bencheikh, and J. A. Levenson, Phys. Rev. A **85**, 023809 (2012).
[22] P. van Loock and A. Furusawa, Phys. Rev. A **67**, 052315 (2003).
[23] R. Y. Teh and M. D. Reid, Phys. Rev. A **90**, 062337 (2014).
[24] F. Gravier and B. Boulanger, J. Opt. Soc. Am. B **25**, 98 (2008).
[25] See Supplemental Material at http://link.aps.org/supplemental/10.1103/PhysRevLett.120.043601 for details on the calculation of the nonseparability criterion S in the case of spontaneous triple-photon generation, details on the validity of the operators expansion, and optical losses simulation.
[26] Z. Y. Ou, S. F. Pereira, H. J. Kimble, and K. C. Peng, Phys. Rev. Lett. **68**, 3663 (1992).